Thermal and mechanical behaviour of crystalline poly(ethylene terephthalate): effects of high temperature annealing and tensile drawing

R. Elenga, R. Seguela* and F. Rietsch
Laboratoire de Structure et Propriétés de l'Etat Solide, URA CNRS 234, Université de Lille I, 59655 Villeneuve d'Ascq Cedex, France
(Received 4 June 1990; revised 19 July 1990; accepted 19 July 1990)

The melting behaviour and several mechanical properties of crystallized poly(ethylene terephthalate) have been investigated paying particular attention to the effect of thermal annealing at high temperature. Although the occurrence of a double melting peak in the differential scanning calorimetry (d.s.c.) curves of isothermally annealed samples can be undeniably ascribed to a recrystallization process during the heating scan, it is suggested that the chain-folded lamellar crystals grown at a moderate crystallization temperature undergo a morphological change into fringed-micelle crystals when submitted to a high temperature annealing. This conclusion is inferred from the striking changes of the mechanical properties of the samples which result from the annealing treatment, in conjunction with the thermal behaviour of drawn samples. This metamorphosis is attributed to ester interchange reactions which turn the chain folds of the amorphous layers into intercrystalline tie molecules at high temperature.

(Keywords: poly(ethylene terephthalate); melting behaviour; mechanical properties; birefringence; shrinkage stress)

INTRODUCTION

The melting behaviour of annealed crystalline poly(ethylene terephthalate) (PET) has been a matter of contradictory interpretations for the past 25 years. Investigations of crystalline PET by means of differential scanning calorimetry (d.s.c.) have often revealed two melting endotherms whose temperature and relative areas depend on the temperature and the duration of the thermal treatment[1–10]. This is not specific to PET since it has been also reported in the case of various polyesters[11–14], as well as for some polyolefins[15,16], polyamides[17,18] and polyethers[19,20]. Generally, only one crystalline form has been observed, indicating that the two melting peaks do not rely on a crystalline modification. Two different interpretations have been proposed for the origin of this phenomenon.

The first interpretation assumes a morphological transformation of the lamellar crystals into bundle-like crystals upon annealing[1–4], the melting of the two types of crystals being respectively associated with the high temperature (HT) and the low temperature (LT) endothermic peaks. Tenants of this proposal have obtained indirect evidence from thermal analyses, infrared measurements, mechanical behaviour and viscoelastic properties on amorphous, annealed or drawn PET. Bell *et al.*[2,3,7] have notably emphasized the analogy between annealed and drawn samples of PET, from both thermal and mechanical standpoints.

The second proposal, which is now the most largely accepted interpretation, is that reorganization of the most defective crystals occurs by gradual melting and immediate recrystallization during the d.s.c. scan until final melting in the HT endothermic peak[21]. The crystals developed during an isothermal crystallization or an annealing treatment melt in the LT endothermic peak. The temperature of the LT peak is closely related to that of the thermal treatment but this is not the case for the HT peak. The first evidence that crystallized PET could partially melt and subsequently recrystallize at high temperatures was given by Zachmann and Stuart[22] (see also ref. 21). More recently, it has been reported that an exothermic crystallization peak may be observed during the course of an isothermal treatment at a temperature between the two melting peaks[5,16] and even during the d.s.c. scan[7,15,19]. Indirect evidence has been also provided through the effect of increasing scanning rate which reduces the HT melting peak area[5,6,11,14,20]. This is relevant to the fact that recrystallization becomes less efficient as the time for recrystallization is reduced.

The controversy mainly lies in the fact that thermal analyses alone can be thoroughly interpreted without making reference to any change in the crystalline morphology brought about by annealing. Notwithstanding this, it is worth noting that poly(butylene terephthalate) (PBT) whose chemical structure is very close to that of PET exhibits a change in morphology depending on the crystallization conditions, without modification of the crystalline structure[23,24]. Two types of usual and unusual spherulites having well separated melting points, 6°C apart, have been clearly observed by optical microscopy and small-angle light scattering[23]. Hence, the occurrence of a morphological change in PET cannot be discarded a priori. Moreover, considering the strong sensitivity of PET's mechanical properties to thermal annealing, this problem deserved reexamination and further investigation.

* To whom correspondence should be addressed

0032-3861/91/111975-08

The purpose of this paper is to show that the two phenomena, i.e. reorganization during the d.s.c. scan and morphological change during annealing, are not basically contradictory and can both contribute to the complex melting behaviour of annealed PET. A chemical origin is given to the morphological modification and concomitant change of mechanical properties upon annealing at HT.

EXPERIMENTAL

Three kinds of PET supplied by Rhône-Poulenc Industries in the form of amorphous films have been studied. The samples, PET1, PET2 and PET3, had the following viscosity average molecular weights $M_v = 27\,000$, 25 000 and 16 000, respectively.

Thermal investigations were performed on a Perkin Elmer DSC-2 differential scanning calorimeter. The calibration of the apparatus for temperature and energy was made by using indium and tin references. The weight of the PET samples was *c.* 6–8 mg and the heating rate was $10°C\,min^{-1}$. The crystal weight fraction of the samples was estimated from the melting enthalpy of perfectly crystalline PET[21], $\Delta H_f^\circ = 140\,J\,g^{-1}$.

The samples used for the mechanical testing, birefringence and shrinkage stress measurements were crystallized at 170°C for 20 h before annealing at 225°C for various lengths of time. The crystallization and annealing treatments were performed in an oven, under nitrogen atmosphere. The dumb-bell test pieces with gauge dimensions 24 × 5 mm were cut from the films and drawn in an Instron tensile testing machine equipped with a heating chamber. The draw rate was either 3.5×10^{-2} or $7 \times 10^{-4}\,s^{-1}$. The actual draw ratio was determined from the displacement of ink marks made on the samples, 1.5 mm apart prior to drawing. The Young's modulus was assessed from the slope of the stress–strain curves recorded at 100°C, using 5 cm long specimens and a $3.5 \times 10^{-4}\,s^{-1}$ strain rate.

Birefringence measurements were carried out on a Leitz polarizing microscope provided with a Ehringhaus compensator.

Shrinkage stress measurements were performed on apparatus developed in the laboratory[25]. The temperature of the experiments was 100°C in order to allow the recovery of the amorphous phase only.

RESULTS AND DISCUSSION

Thermal behaviour of isotropic samples

In contrast to PET1 and PET3, PET2 regularly displayed a tiny but sharp crystallization exotherm between the usual two melting peaks, after annealing at high temperature. An examination of the data in the literature[1–21] shows that this phenomenon is an exception rather than a rule. Moreover, it does not seem to be relevant to a higher resolution of the thermogram since neither the scanning rate nor the sample thickness have a determining influence on it. However, one could suspect an effect of some additives liable to modify the kinetics of the recrystallization process. Notwithstanding the lack of a conclusive explanation for this phenomenon, our results are consistent with the classical scheme of melting and recrystallization discussed above, even when no exotherm is observed. *Figure 1* shows the d.s.c. heating curves of PET1 samples annealed for various times at 225°C after an isothermal crystallization at 170°C from the glassy state. The LT peak which results from the melting of the crystals reorganized at the annealing temperature grows steadily with increasing annealing time. The HT endotherm which arises from the melting of the crystals reformed after occurrence of the LT peak decreases in parallel. This is a consequence of the reduced capability of the material to recrystallize above the LT peak as the peak is shifted towards higher temperatures. *Figure 2* shows two schematic d.s.c. curves which simulate the experimental curves (b) and (d) of *Figure 1* together with the hypothetical curves for the three basic components, that is the melting of the annealed crystals (m.a.c.) followed by a partial recrystallization (p.r.) and the final melting of the recrystallized fraction (m.r.f.). The area of the m.a.c. peak is equal to that of the overall d.s.c. curve and the area of the p.r. peak is equal to that of the m.r.f. peak. The shape of the p.r. curves reflects the fact that the recrystallization rate becomes very low above 245°C[21,22].

The upward temperature shift of the LT peak which takes place as the annealing time increases provides evidence for a second stage in the reorganization process which has often been assumed to be a surface smoothing of the crystals[6,8,21,26–28] as judged from wide-angle and small-angle X-ray measurements. Indeed, surface smoothing is expected to reduce the surface free energy

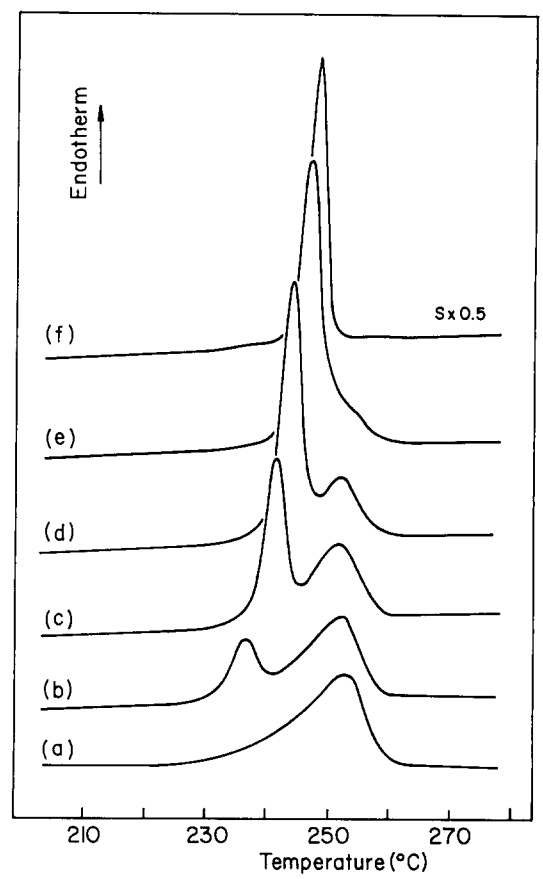

Figure 1 D.s.c. melting curves of PET1 samples crystallized from the glassy state at 170°C for 20 h and subsequently annealed at 225°C for various times, t_a (α_c is the crystal weight fraction): (a) $t_a = 0$ min, $\alpha_c = 0.40$; (b) $t_a = 15$ min, $\alpha_c = 0.41$; (c) $t_a = 45$ min, $\alpha_c = 0.43$; (d) $t_a = 90$ min, $\alpha_c = 0.45$; (e) $t_a = 180$ min, $\alpha_c = 0.46$; (f) $t_a = 420$ min, $\alpha_c = 0.48$

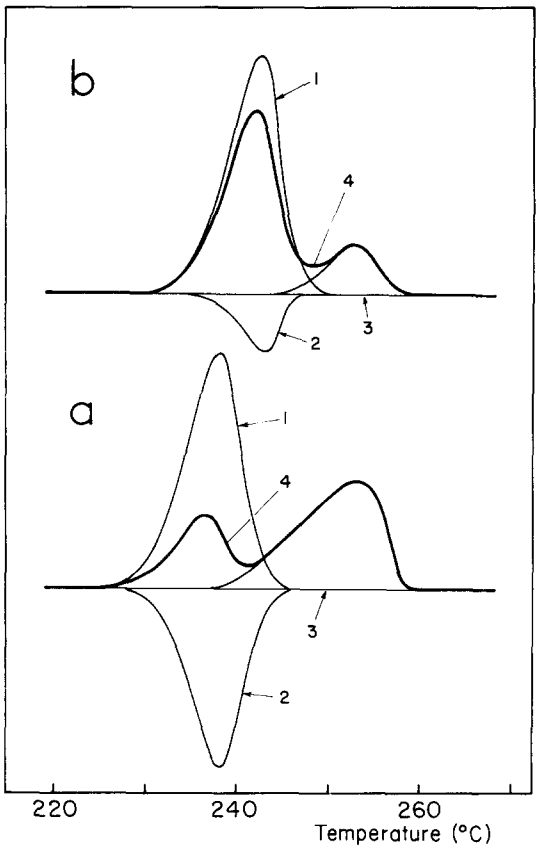

Figure 2 Schematic construction of the d.s.c. heating curves of crystalline PET1 samples annealed at 225°C for (a) $t_a = 15$ min and (b) $t_a = 90$ min. Curve 1 is the melting of the annealed crystals, curve 2 is the recrystallization process, curve 3 is the melting of the recrystallized fraction and curve 4 is the resulting d.s.c. curve (see *Figure 1b* and *d* for comparison)

due to the relaxation of internal stresses and removal of surface imperfections, thus leading to an increase of the melting point of the crystals at constant thickness. From the standpoint of kinetics, the data of Zachmann and Stuart[22] show that only a few minutes are required for the complete restoration of the crystalline phase after the melting of the imperfect crystals grown from cold crystallization. On the other hand, the process of crystal perfecting takes place over several hours and exhibits a maximum rate at *c.* 180–200°C, as shown by Alfonso *et al.*[27] and Lin and Koenig[9] from the time dependence of the LT peak temperature shift. This comparison emphasizes that crystal reorganization is a complex phenomenon involving at least two different processes.

The melting behaviour of samples isothermally crystallized from the melt also deserves examination. *Figure 3* shows the d.s.c. curves of PET1 samples recorded on heating directly from the crystallization temperature, $T_c = 225$°C, without previous cooling. For crystallization times $t_c < 30$ min, only the HT melting peak appears which grows in size as t_c increases. The LT melting peak arises for $t_c \approx 30$ min, then it grows with increasing t_c and gradually merges into the HT peak. At first sight, this is consistent with the model assuming a morphological change of the HT melting crystals into the LT melting ones. However, upon further examination, the above results can be analysed through the melting–recrystallization scheme, considering that the absence of the LT peak for short crystallization periods is relevant to the fast kinetics of the reorganization in the range 230–240°C[21,22]. In this instance, the whole crystalline part of the isothermally crystallized material is involved in the recrystallization process, but no additional amorphous material is allowed to crystallize during the d.s.c. scan. In other words, the recrystallization mechanism is much faster than the primary crystallization. Further evidence for this comes from the fact that recrystallization above the LT melting peak, during the d.s.c. scan, occurs within an interval shorter than the duration of the isothermal crystallization from the melt. The reason for this is the melting and recrystallization processes take place simultaneously, the recrystallization of the chains which melt at the beginning of the LT peak (i.e. the less perfect or thinner crystals) being promoted on the surfaces of the crystals which melt at the end of the LT peak (i.e. the more perfect or thicker crystals). Alternatively, studying the double melting behaviour of poly(aryl-ether-ether-ketone), Lee and Porter[29] have proposed that some core portion of the original crystals is preserved from melting until the end of the recrystallization process.

Thermal behaviour of drawn samples

Figure 4 shows the melting curves of PET3 samples isothermally crystallized at $T_c = 170$°C and uniaxially drawn at $T_d = 125$°C. The emergence and gradual growth of a second melting endotherm on the LT side of the original HT melting peak as a function of the draw ratio seems to be a logical consequence of the fibrillar

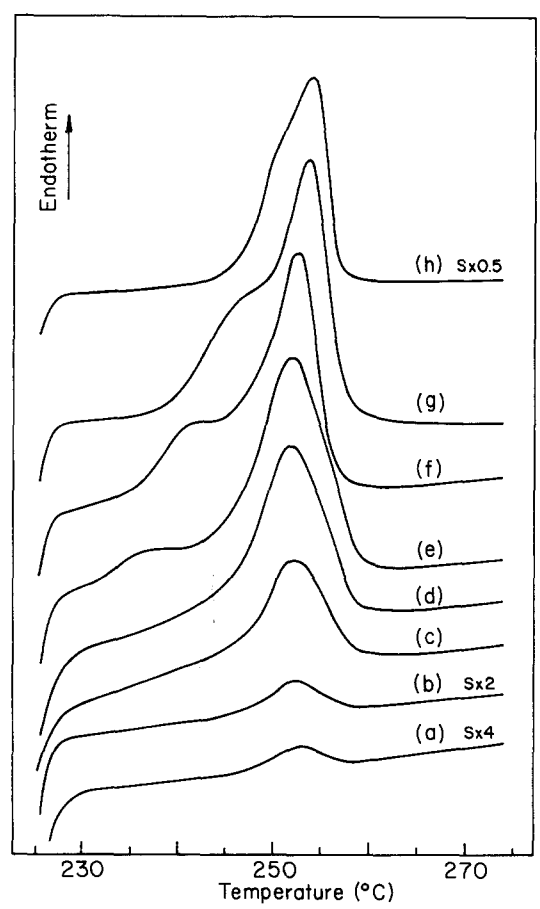

Figure 3 D.s.c. melting curves of PET1 samples crystallized from the melt at 225°C for various times, t_c: (a) $t_c = 1$ min; (b) $t_c = 2$ min; (c) $t_c = 5$ min; (d) $t_c = 15$ min; (e) $t_c = 30$ min; (f) $t_c = 60$ min; (g) $t_c = 120$ min; (h) $t_c = 180$ min (S is the sensitivity of the d.s.c. recorder)

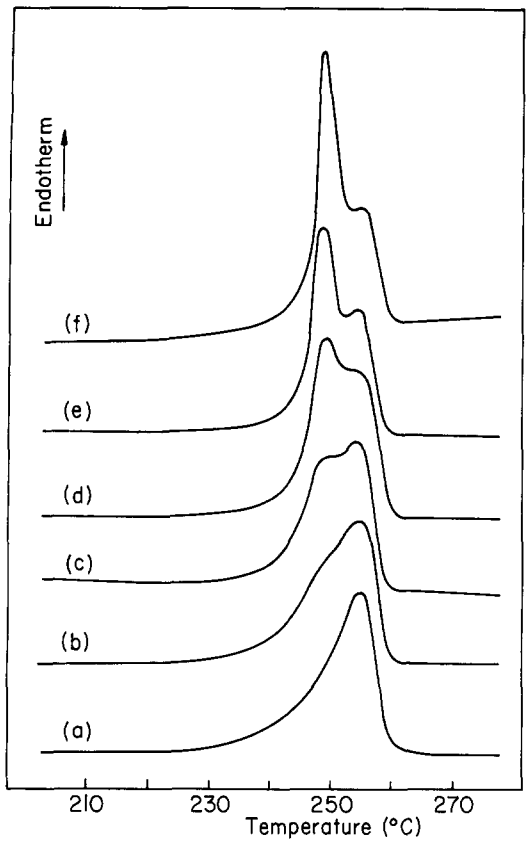

Figure 4 D.s.c. melting curves of PET3 samples crystallized for 20 h at 170°C and subsequently drawn at 125°C, as a function of the draw ratio, λ: (a) $\lambda=2.3$, $\alpha_c=0.40$; (b) $\lambda=4.0$, $\alpha_c=0.42$; (c) $\lambda=4.5$, $\alpha_c=0.43$; (d) $\lambda=5.0$, $\alpha_c=0.45$; (e) $\lambda=5.5$, $\alpha_c=0.46$; (f) $\lambda=6.2$, $\alpha_c=0.48$ ($\dot{\varepsilon}=3.5\times10^{-2}\,s^{-1}$)

transformation, as pointed out by Yubayashi *et al.*[30]. This typical transformation of semi-crystalline polymers under tensile drawing involves a change of the chain-folded crystalline structure of the isotropic material into a fringed-micelle structure due to the unfolding mechanism of the chains. An alternative interpretation has been proposed by Fakirov *et al.*[31] who assumed that double melting peaks for heat-set PET fibres are relevant to the melting and partial recrystallization during the d.s.c. heating scan of the crystals reorganized during the isothermal treatment, as is the case for annealed isotropic PET. However, Gupta *et al.*[32] have suggested that double melting occurs as long as part of the original structure remains in the fibres, the original part undergoing reorganization during scanning. In this connection, an HT exothermic peak during the d.s.c. scanning of drawn PET fibres has been reported by Vallat *et al.*[33]. These authors claimed that the exothermic effect resulted from the release of stored mechanical energy as the sample softened in the melting temperature range rather than from a recrystallization process above the LT melting peak. Besides, from the standpoint of kinetics, recrystallization of the LT melting crystals into more stable crystals during the d.s.c. scan of drawn samples seems unlikely considering the LT peak always occurs at a temperature >245°C (*Figure 4*, refs. 31–33) where the recrystallization rate is very low[21]. Evidence for this is shown in *Figure 1* where the HT peak due to recrystallization in isotropic PET1 disappears when the LT peak is shifted >245°C. Therefore, the interpretation of the double melting in terms of morphological change induced by drawing appears more appropriate. In this instance, the LT peak is ascribed to the fringed-micelle crystals built up by chain unfolding and the HT peak corresponds to the untransformed fraction of the lamellar crystals which can undergo reorganization during the heating scan, as is the case for isotropic samples.

The study of PET samples drawn from the amorphous state is of value for understanding the thermal behaviour of crystalline samples. Indeed, a double melting endotherm is also observed in the case of amorphous PET drawn beyond the neck in the temperature range of the glass transition. Despite the low molecular mobility at the glass transition temperature, crystallization upon drawing is allowed by the strain-induced orientation of the chains which improves the crystallization kinetics in comparison to isotropic samples[34]. *Figure 5* displays the d.s.c. curves of PET3 fibres having similar draw ratios, for different values of the draw temperature. The HT peak area is clearly improved at the expense of the LT peak area when T_d increases, the temperature of each peak being unchanged. This result is obviously not related to an annealing effect during the drawing process but it can be associated with a morphological change. Indeed, drawing at a temperature below the glass transition enforces a fringed-micelle crystallization of the cold-oriented chains, but increasing the drawing temperature activates the relaxation and disentanglement of the oriented amorphous chains during the drawing process as previously suggested by Engelaere *et al.*[35]. This is supported by small-angle neutron scattering measurements which show that the deformation of PET below the glass transition is not affine on the molecular scale, i.e. the molecular draw ratio is significantly lower than the macroscopic draw ratio[36]. Owing to this relaxation capability, the molecules can undergo chain-folded crystallization during the draw process and give rise to rather imperfect lamellar crystals liable to reorganize when subjected to the heating scan of the d.s.c. analysis. Moreover, the higher the draw temperature, the greater

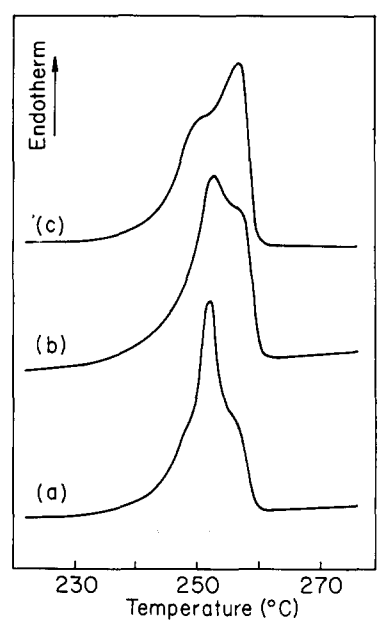

Figure 5 D.s.c. melting curves of PET3 samples drawn from the glassy state for three values of the draw temperature, T_d: (a) $T_d=55°C$, $\lambda=4.8$; (b) $T_d=65°C$, $\lambda=4.6$; (c) $T_d=80°C$, $\lambda=4.8$ ($\dot{\varepsilon}=3.5\times10^{-2}\,s^{-1}$)

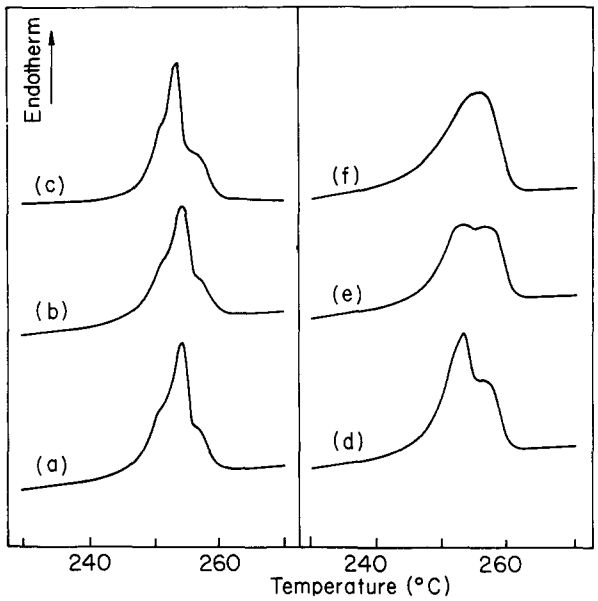

Figure 6 D.s.c. melting curves of PET2 samples drawn from the glassy state for two values of the draw rate, $\dot{\varepsilon}$, and three values of the draw temperature, T_d: $\dot{\varepsilon}=3.5\times10^{-2}\ s^{-1}$ (a) $T_d=55°C$, $\lambda=5.4$, (b) $T_d=65°C$, $\lambda=5.4$, (c) $T_d=85°C$, $\lambda=5.1$; $\dot{\varepsilon}=7\times10^{-4}\ s^{-1}$ (d) $T_d=55°C$, $\lambda=4.4$, (e) $T_d=65°C$, $\lambda=4.4$, (f) $T_d=85°C$, $\lambda=4.4$

is the trend to chain-folded crystallization, due to a higher chain mobility in the fibre. Therefore, the d.s.c. curves in *Figure 5* agree with the LT and HT peaks being assigned to the fringed-micelle and chain-folded crystals as has been done for results on drawn crystalline samples.

The effect of the molecular weight on the thermal behaviour of samples drawn from the glassy state supports the above conclusion. This is emphasized by the study of PET2 which has a higher molecular weight than PET3. The d.s.c. curves of PET2 (*Figure 6a–c*) exhibit no conspicuous influence of the draw temperature at a draw rate $\dot{\varepsilon}=3.5\times10^{-2}\ s^{-1}$. However, when the draw rate is reduced by a factor 50, striking changes appear in the d.s.c. curves of PET2 samples drawn from the glass (*Figure 6d–f*). These changes are similar to those previously observed in the d.s.c. curves of PET3, for the same range of draw temperature but for a greater draw rate (*Figure 5*). The reason for this lies in the fact that long range molecular motions are much slower in PET2 because of a higher molecular weight (i.e. a higher viscosity) so that a very low draw rate is required to allow chain relaxation and disentanglement. This statement is based on the observation by Engelaere *et al.*[35] that the drawing behaviour of an amorphous PET sample of molecular weight $M_v=18\,800$ departs much more from that of a permanent polymer network than a sample with $M_v=26\,000$, when the draw rate is $\dot{\varepsilon}=8\times10^{-4}\ s^{-1}$ and $T_d=80°C$. Therefore, as in the case of PET3, the build up of an HT peak in the melting curves of drawn PET2 samples can be ascribed to the activation of a chain-folded crystallization process due to chain relaxation at the expense of the fringed-micelle crystallization enforced by chain orientation, the main difference between the two samples being the time scale of the process.

Mechanical properties

The effect of thermal annealing on the mechanical properties of crystallized PET has been investigated through tensile drawing behaviour. *Figure 7* shows the nominal stress–strain curves of PET3 samples annealed for various lengths of time at $T_a=225°C$. Similar curves have been obtained for PET1 samples with a small difference in stress level. Annealing brings about a drastic loss of drawability together with a significant increase in strength at yield. This is all the more remarkable since crystallinity hardly changes in the range of annealing time investigated. In parallel, it is quite interesting to note that the modulus which mainly depends on the crystal level is practically insensitive to the annealing treatment (*Figure 8*). All these features are relevant to a morphological change in crystalline PET from a ductile form into a brittle one as a result of HT annealing. It is suspected that the chain-folded lamellar crystals initially grown during the isothermal crystallization at $T_c=170°C$ turn into fringed-micelle crystals during the annealing

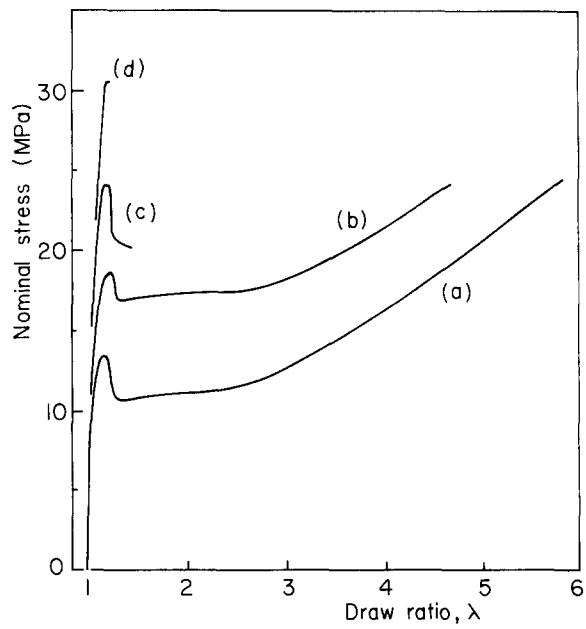

Figure 7 Stress–strain curves at 125°C of PET3 samples crystallized and annealed at 225°C, as a function of the annealing time, t_a: (a) $t_a=0$ min; (b) $t_a=15$ min; (c) $t_a=180$ min; (d) $t_a=300$ min

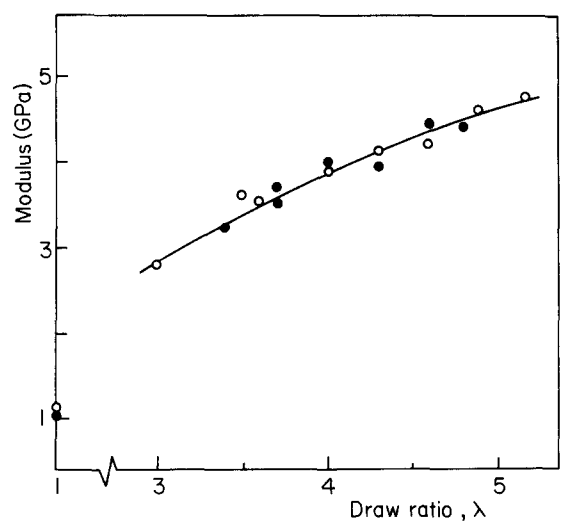

Figure 8 Young's modulus at 100°C of crystallized PET3 samples as a function of the draw ratio, λ: (○) without annealing; (●) after annealing at 225°C for 15 min

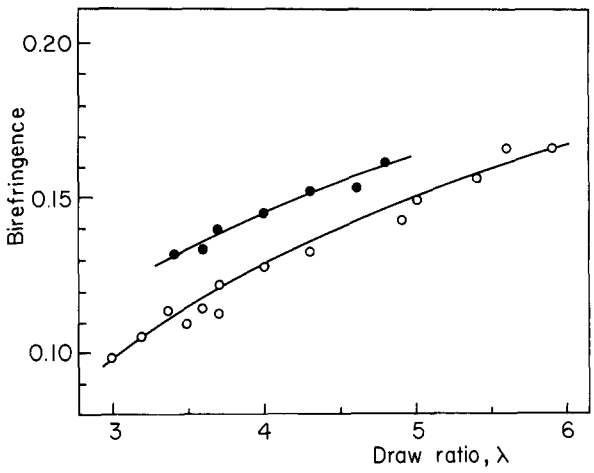

Figure 9 Birefringence of crystallized PET3 samples as a function of the draw ratio, λ: (○) without annealing; (●) after annealing at 225°C for 15 min

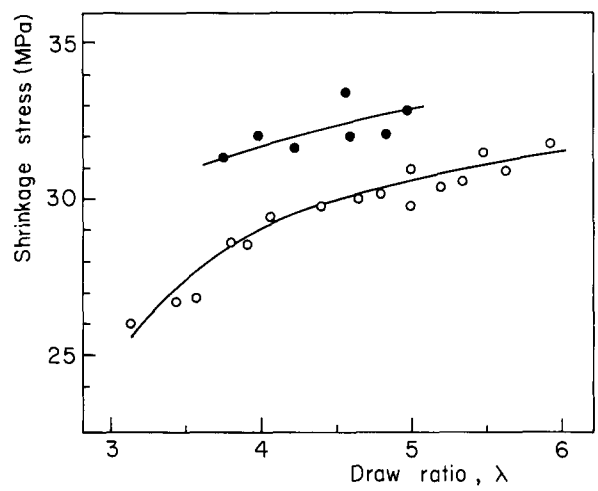

Figure 10 Shrinkage force at 100°C of crystallized PET3 samples as a function of the draw ratio, λ: (○) without annealing; (●) after annealing at 225°C for 15 min

step. Indeed, this latter form has less potential drawability than the former because of the partially unfolded macroconformation of the chains. This has been illustrated by Holdsworth and Keller[37] and Domzy *et al.*[38] on ethylene copolymers which exhibit a considerably improved drawability when a high degree of regular chain folding is realized by means of a dilute solution crystallization method of preparation.

According to Schultz[39], fringed-micelle crystals should be more ductile than chain-folded crystals due to the large number of tie molecules transmitting the load homogeneously to the crystals and allowing them to flow plastically instead of being brittle. This statement, which could appear to contradict the previous argument, is concerned with the microstructural aspects of failure of the crystals in relation to the yielding behaviour of semicrystalline polymers, and not with the mechanisms of large deformations. On the other hand, our conclusion has additional experimental support. For the same draw ratio, the birefringence of annealed crystalline samples is significantly greater than that of non-annealed samples, as shown in *Figure 9* for PET3. *Figure 10* shows that the shrinkage force of fibres measured at 100°C is greater for the annealed rather than the non-annealed samples, for PET3 samples drawn up to the same draw ratio. Similar results have been recorded from PET1 crystalline samples using both birefringence and shrinkage force measurements. These data are a strong indication that a larger number of tie molecules cross the amorphous phase of crystalline PET after an annealing treatment at $T_a = 225$°C. This is in perfect agreement with the change of the chain-folded crystals into fringed-micelle crystals.

Metamorphosis model

There is no obvious physical reason for the morphological change of crystalline PET from a ductile to a brittle form upon annealing without significant change in the crystallinity. However, there may be a chemical origin to this phenomenon owing to the transesterification reactions. Indeed, such reactions are known to occur in molten PET[40] but they also take place in the amorphous phase of semicrystalline PET >200°C, as demonstrated by chemical analyses[41], healing phenomena[42] and small-angle neutron scattering[43]. Transesterification reactions have been already claimed to help remove crystal surface imperfections[8]. Indeed, strained amorphous chains may open and recombine into unconstrained chains which allow crystal perfecting near the surface. However, chain folds are liable to be changed into tie molecules with little probability of reverting to folds for conformational reasons. This is illustrated in *Figure 11* which shows molecular models for an ester–ester interchange reaction between neighbouring chain folds and for an hydroxyl–ester interchange reaction between chain end and chain fold. Experimental evidence has been provided by Miyagi and Wunderlich[44] who showed that, after hydrolysis of crystalline PET, an annealing treatment >200°C gives rise to chain-extended rather than chain-folded crystals. Additional support for our proposal is that polymeric selenium (Se) has been recognized to form chain-extended crystals from lamellar crystals by opening chain folds and reconnecting broken bonds belonging to adjacent lamellae[45,46], owing to the labile character of the Se–Se bond. Polyamide 6 is also thought to undergo transformation from lamellar to chain-extended crystals under HT and high pressure treatment due to transamidation reactions within the amorphous layers[47].

The chain topology in semicrystalline PET before and after annealing at HT is given in *Figure 12*, taking into consideration the transesterification reactions discussed above. The loose chain folds and tie molecules form the

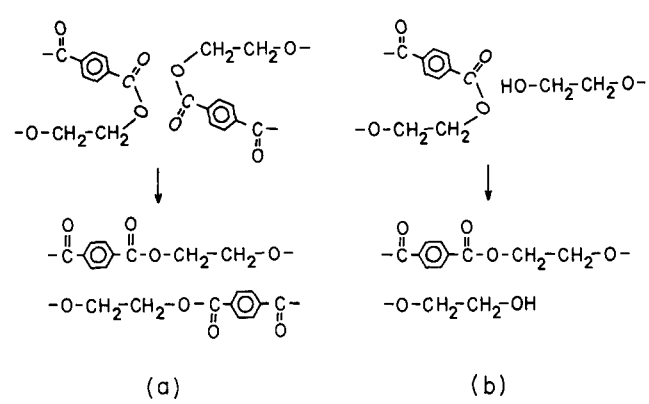

Figure 11 Molecular models for the ester–ester (a) and ester–hydroxyl (b) interchange reactions in PET

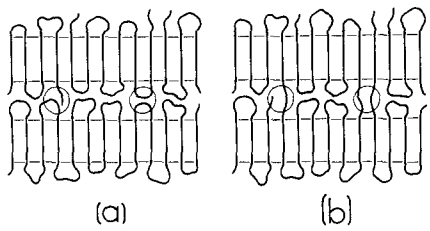

Figure 12 Topological model of the chain rearrangement in crystalline PET as a result of transesterification in the amorphous phase during HT annealing: (a) before annealing; (b) after annealing

amorphous component of the model. *Figure 12* shows that the chemical chain rearrangements in the amorphous layers involve a morphological change of the crystals from chain-folded lamellae into fringed micelles which accounts for the drastic loss of drawability of the bulk material after annealing. Indeed, chain-folded crystals are much more prone to give high draw ratios than fringed-micelle crystals owing to the chain unfolding mechanism which can only operate in the chain-folded crystals. Moreover, the greater the number of tie molecules in the isotropic sample, the stronger will be the chain orientation after drawing at a given draw ratio.

Solid phase polycondensation through water or glycol elimination also occurs in PET at HT and could contribute to the change of properties measured on the drawn samples (see *Figures 9* and *10*). However, according to the study by Droscher and Wegner[48], the molecular weight increase due to a 15 min annealing at 225°C does not exceed 10%. Besides, it has been clearly pointed out that transesterification is much more efficient than polycondensation in the solid state[42,44].

CONCLUSIONS

Imperfect lamellar crystals grown upon isothermal crystallization of glassy PET at LT (cold crystallization) are likely to be transformed into fringed-micelle crystals during annealing at HT, owing to the ester interchange reactions which turn chain folds into intercrystalline tie molecules. This chemically induced metamorphosis provides a satisfactory explanation for the drastic loss of drawability of crystalline PET upon annealing for long time periods at nearly constant crystallinity.

The model proposed above is consistent with a melting and recrystallization process during the heating scan of the d.s.c. analyses. Indeed, the surface free energy of chain-folded crystals is lower than that of fringed-micelle crystals, as estimated from the calculation of the entropic contributions of the amorphous chains[49]. Therefore, a thermodynamically governed growth of more stable chain-folded crystals is expected to take place after melting of the fringed-micelle crystals provided there is sufficient time for recrystallization to occur, i.e. if the melting point of the annealed crystals is far below the thermodynamic melting point or if the scanning rate is low.

An interesting point is the similarity reported by Bell *et al.*[2,3,7] between crystalline PET and polyamide 66, from both thermal and mechanical standpoints. In this connection, we have previously indicated that the transamidation-prone polyamides are thought to undergo a change from chain-folded crystals into fringed-micelle crystals when submitted to a HT annealing. This is all the more remarkable if one considers the strong reduction of the drawability[2] of polyamide 66 after an annealing treatment at HT. This particular behaviour of polyamides constitutes a striking parallel with the present work in which chain interchange reactions are given a prime role in the morphological and mechanical modifications of crystalline PET upon HT annealing.

REFERENCES

1 Mitsuishi, Y. and Ikeda, M. J. *J. Polym. Sci., Polym. Phys. Edn.* 1966, **4**, 283
2 Bell, J. P. and Dumbleton, J. H. *J. Polym. Sci., Polym. Phys. Edn.* 1969, **7**, 1033
3 Bell, J. P. and Murayama, T. *J. Polym. Sci., Polym. Phys. Edn.* 1969, **7**, 1059
4 Nealy, D. L., Davis, T. G. and Kibler, C. J. *J. Polym. Sci., Polym. Phys. Edn.* 1970, **8**, 2141
5 Roberts, R. C. *J. Polym. Sci., Polym. Lett. Edn.* 1970, **8**, 381
6 Holdsworth, P. J. and Turner-Jones, A. *Polymer* 1971, **12**, 195
7 Sweet, G. E. and Bell, J. P. *J. Polym. Sci., Polym. Phys. Edn.* 1972, **10**, 1273
8 Groeninckx, G. and Reynaers, H. *J. Polym. Sci., Polym. Phys. Edn.* 1980, **18**, 1325
9 Lin, S. B. and Koenig, J. L. *J. Polym. Sci., Polym. Symp.* 1984, **71**, 121
10 Zhou, C. and Clough, S. B. *Polym. Eng. Sci.* 1988, **28**, 65
11 Hobbs, S. Y. and Pratt, C. F. *Polymer* 1975, **16**, 462
12 Marrs, W., Peters, R. H. and Still, R. H. *J. Appl. Polym. Sci.* 1979, **23**, 1077
13 Rim, P. B. and Runt, J. P. *Macromolecules* 1983, **16**, 762
14 Yeh, J. T. and Runt, J. *J. Polym. Sci., Polym. Phys. Edn.* 1989, **27**, 1543
15 Lemstra, P. J., Kooistra, T. and Challa, G. J. *J. Polym. Sci., Polym. Phys. Edn.* 1972, **10**, 823
16 Kamide, K. and Yamaguchi, K. *Makromol. Chem.* 1972, **162**, 205
17 Bell, J. P., Slade, P. E. and Dumbleton, J. H. *J. Polym. Sci., Polym. Phys. Edn.* 1968, **6**, 1773
18 Ceccorulli, G., Manescalchi, F. and Pizzoli, M. *Makromol. Chem.* 1975, **176**, 1163
19 Jaffe, M. and Wunderlich, B. *Kolloid-Z. Z. Polym.* 1968, **216–217**, 203
20 Lee, Y., Porter, R. S. and Lin, J. S. *Macromolecules* 1989, **22**, 1756
21 Wunderlich, B. 'Macromolecular Physics, Vol. 3: Crystal Melting', Academic Press, New York, 1980, Ch. 9
22 Zachmann, H.-G. and Stuart, H. A. *Makromol. Chem.* 1960, **41**, 131, 148
23 Stein, R. S. and Misra, A. *J. Polym. Sci., Polym. Phys. Edn.* 1980, **18**, 327
24 Ludwig, H. J. and Eyerer, P. *Polym. Eng. Sci.* 1988, **28**, 143
25 Engelaere, J.-C., Cavrot, J.-P. and Rietsch, F. *Eur. Polym. J.* 1980, **16**, 721
26 Coppola, G., Fabbri, P., Alfonso, G. C., Dondero, G. and Pedemonte, E. *Makromol. Chem.* 1975, **176**, 767
27 Alfonso, G. C., Pedemonte, E. and Ponzetti, L. *Polymer* 1979, **20**, 104
28 Fontaine, F., Ledent, J., Groeninckx, G. and Reynaers, H. *Polymer* 1982, **23**, 185
29 Lee, Y. and Porter, R. S. *Macromolecules* 1987, **20**, 1336
30 Yubayashi, T., Orito, Z. and Yamada, N. *J. Chem. Soc. Jpn* 1966, **69**, 1798
31 Fakirov, S., Fischer, E. W., Hoffmann, R. and Schmidt, G. F. *Polymer* 1977, **18**, 1121
32 Gupta, V. B., Ramesh, C. and Gupta, A. K. *J. Polym. Sci., Polym. Phys. Edn.* 1984, **29**, 3727
33 Vallat, M.-F., Plazek, D. J. and Bhushan, B. *J. Polym. Sci., Polym. Phys. Edn.* 1988, **26**, 555
34 Le Bourvellec, G., Monnerie, L. and Jarry, J. P. *Polymer* 1987, **28**, 1712
35 Engelaere, J.-C., Cavrot, J.-P. and Rietsch, F. *Polymer* 1982, **23**, 766
36 Gilmer, J. W., Wiswe, D., Zachmann, H.-G., Kugler, J. and Fischer, E. W. *Polymer* 1986, **27**, 1391
37 Holdsworth, P. J. and Keller, A. *J. Polym. Sci., Polym. Phys. Edn.* 1968, **6**, 707

38 Domzy, R. C., Alamo, R., Mathieu, P. J. M. and Mandelkern, L. *J. Polym. Sci., Polym. Phys. Edn.* 1984, **22**, 1727
39 Schultz, J. M. *Polym. Eng. Sci.* 1984, **24**, 770
40 Davies, T. in 'Chemical Reactions of Polymers' (Ed. E. M. Fettes), Wiley-Interscience, New York, 1964, Ch. VII
41 Dröscher, M. and Schmidt, F. G. *Polym. Bull.* 1981, **4**, 261
42 Fakirov, S. *J. Polym. Sci., Polym. Phys. Edn.* 1984, **22**, 2095
43 McAlea, K. P., Schultz, J. M., Gardner, K. H. and Wignall, G. D. *Polymer* 1986, **27**, 1581
44 Miyagi, A. and Wunderlich, B. *J. Polym. Sci., Polym. Phys. Edn.* 1972, **10**, 2085
45 Crystal, R. G. *J. Polym. Sci., Polym. Phys. Edn.* 1970, **8**, 2153
46 Coughlin, M. C. and Wunderlich, B. *Kolloid-Z. Z. Polym.* 1972, **250**, 482
47 Gogolewski, S. *Polymer* 1977, **18**, 63
48 Dröscher, M. and Wegner, B. *Polymer* 1978, **19**, 43
49 Wunderlich, B. 'Macromolecular Physics, Vol. 2: Crystal Nucleation, Growth, Annealing', Academic Press, New York, 1976, Ch. 5